Imaging spectroscopy of hard x-ray sources in solar flares using regularized analysis of source visibilities

Journal of Physics: Conference Series **124** (2008) 012034 doi:10.1088/1742-6596/124/1/012034

Imaging spectroscopy of hard x-ray sources in solar flares using regularized analysis of source visibilities

A M Massone[1], M Piana[2] and M Prato[3]

[1] CNR - INFM LAMIA, via Dodecaneso 33, I-16146 Genova, Italy
[2] Dipartimento di Informatica, Università di Verona, Ca' Vignal 2, Strada le Grazie 15, I-37134 Verona, Italy
[3] Dipartimento di Matematica e Applicazioni, Università di Modena e Reggio Emilia, Via Campi 213/b, Modena, I-41100, Italy

E-mail: massone@ge.infm.it

Abstract. The Reuven Ramaty High-Energy Solar Spectroscopic Imager (RHESSI) uses rotational modulation synthesis for imaging hard X-ray flares with unprecedented spatial and spectral resolution. As the spacecraft rotates, imaging information is encoded as rapid time-variations of the detected flux. We introduce a novel method for imaging spectroscopy analysis of hard X-ray emission which reconstructs electron flux maps at different energies involving regularized inversion of X-ray count visibility spectra (i.e., direct, calibrated measurements of specific Fourier components of the source spatial structure). Starting from the reconstructed electron images it is possible to extract and compare electron flux spectra from different regions, which is a crucial step for the comprehension of the acceleration mechanisms during the solar flare.

1. Introduction

The only practical method of obtaining ∼arc-second angular resolution in hard X-ray emission by solar surface within the cost, mass, and launch constraints of a small satellite is to use Fourier transform imaging [11]. One of the most powerful Fourier techniques is rotational modulation synthesis, first proposed by Mertz [8] and implemented by Schnopper *et al* [12]. This idea is at the basis of the Reuven Ramaty High Energy Solar Spectroscopic Imager (RHESSI), which uses nine collimators, each consisting of a pair of widely separated grids (each pair with a different pitch) in front of a germanium detector, to modulate the X-ray emission during solar flares [5]. The combined effect of the spacecraft rotation and the flux modulation of the grids is that, for each X-ray count energy, the data provided by RHESSI are a set of calibrated measurements of spatial Fourier components of the source distribution (called *visibilities*) sampled at particular pairs of spatial frequencies.

Since its launch on February 5, 2002, one of the main goals of the RHESSI mission has been to combine high-resolution imaging in hard X-rays with high resolution spectroscopy in order to obtain a detailed energy spectrum at each point of the image. In the last years several image processing techniques (e.g., back projection, CLEAN, Maximum Entropy, Pixon) have been studied and developed in order to obtain two-dimensional maps of X-ray emission at different energies. On the other hand, starting from X-ray count flux spectra, reliable reconstructions of the mean electron distribution in the plasma (that produces X-ray emission

through Bremsstrahlung) can be obtained by means of regularization approaches with penalty terms of different nature. So far, typical imaging spectroscopy techniques have combined these tools according to the following scheme: a) starting from the measured visibilities, build a set of X-ray count images of the source at different energies; b) select one or more regions of interest in the X-ray count maps; c) for each X-ray count map, extract the flux from the regions selected in b) by integrating the pixels values; d) build the X-ray count flux spectra (one for each region) as a function of energy; e) reconstruct the corresponding electron flux spectra through a regularized inversion of the integral equation linking the X-ray count with the electron spectra.
What we want to do now is to face the imaging spectroscopy problem in a different way: we propose a method which is able to produce spatial maps of the electron flux for any given electron energy. Once these electron maps are available, electron flux spectra from local regions can be straightly extracted and compared. This goal can be achieved in two different ways: the first one is a limit case of the traditional method previously described in which each pixel of the image represents a region of interest. The electron flux spectrum of each pixel is therefore reconstructed leading to an electron flux map for each energy. This approach has two main drawbacks. The first one is the extremely high computational cost of the algorithm due to the huge number of regularized inversions required (one for each pixel of the map). The second one concerns the numerical instability of the method. The problem is that the content of each pixel of the X-ray count maps is the result of the application of an image reconstruction method to the visibilities given by RHESSI. Therefore, the inversion procedure described in e) is not performed on direct measurements but on data which have already passed through a processing step. This fact can lead to the presence of unphysical artifacts in the final electron images despite regularization. The method we propose (see [9]) avoids both drawbacks: the regularized inversion in the energy direction is straightly performed on the X-ray count visibilities and, for each electron energy, a set of regularized electron visibilities is obtained. Then, Fourier-based imaging techniques are applied to these reconstructed electron visibilities to obtain the two-dimensional electron flux maps at different energies.
This technique has two main advantages: first, to utilize as input data for the inversion the X-ray count visibilities, which are the best measurements available in the RHESSI framework; then, to impose a certain level of smoothness in the electron energy direction, thus avoiding the unphysical artifacts produced by traditional imaging spectroscopy methods which build up each X-ray count image independently and without any spectral correlation.

2. Description of the method

RHESSI encodes the information coming from a spatial flux distribution in the sun in two different but equivalent ways: on the one hand, the X-ray counts detected by RHESSI are labelled according to their energy and their detection time so that a time profile for a fixed energy and a X-ray count spectrum for a fixed time interval are available. On the other hand, through the knowledge of the geometry and the hardware of the spacecraft it is possible to connect each time point, and therefore each X-ray count detected by each RHESSI collimator, to a pair of angles (named *roll angle* and *aspect phase*) related to the position of the source with respect to a particular system of coordinates fixed on the collimator itself. This characterization of the X-ray counts allows to stack the data using spacecraft roll angles and aspect phases making long data sets equivalent to a single rotation. The result of this combination is that, after a pre-processing step, measurements of the Fourier transform of the X-ray count flux sampled at specific pairs of spatial frequencies are achieved. Formally, for each one of the nine RHESSI detectors, the visibility $V(u,v;q)$ at spatial frequencies (u,v) and X-ray count energy q is defined as

$$V(u,v;q)dq = \int_x \int_y \int_{\epsilon=q}^{\infty} D(q,\epsilon) I(x,y;\epsilon) e^{2\pi i(ux+vy)} d\epsilon dx dy, \qquad (1)$$

where $D(q,\epsilon)$ is the entry of the Detector Response Matrix (DRM) at X-ray count energy q and photon energy ϵ and $I(x,y;\epsilon)$ is the unknown map of the emitted X-rays. The matrix DRM is known from the hardware of the spacecraft and accounts for all the instrumental effects that the presence of the couple of grids and the detector have on a photon which incides the front grid of the collimator before being recorded by RHESSI. Let us denote the local density of target particles along line-of-sight depth $\ell(x,y)$ with $n(x,y,z)$ and the differential electron flux spectrum at the point (x,y,z) in the source with $F(x,y,z;E)$. Then it is well-known [3] that the process that relates $F(x,y,z;E)$ and the corresponding photon distribution $I(x,y;\epsilon)$ is essentially collisional Bremsstrahlung and is described by the integral equation

$$I(x,y;\epsilon)=\frac{1}{4\pi R^2}\int_{E=\epsilon}^{\infty}\int_{z=0}^{\ell(x,y)} n(x,y,z)F(x,y,z;E)Q(\epsilon,E)dzdE, \tag{2}$$

where $R=1$ AU and $Q(\epsilon,E)$ is the Bremsstrahlung cross-section which we will assume according to formula 3BN in the Koch and Motz 1959 paper [6], i.e., isotropic, fully relativistic with Coulomb correction at small energies.
If we define the electron flux spectrum image $N(x,y)\overline{F}(x,y;E)$ by

$$N(x,y)\overline{F}(x,y;E)=\int_{z=0}^{\ell(x,y)} n(x,y,z)F(x,y,z;E)dz, \tag{3}$$

where the column density at each point (x,y) in the image is given by

$$N(x,y)=\int_{z=0}^{\ell(x,y)} n(x,y,z)dz, \tag{4}$$

then we may write

$$I(x,y;\epsilon)=\frac{1}{4\pi R^2}\int_{E=\epsilon}^{\infty} N(x,y)\overline{F}(x,y;E)Q(\epsilon,E)dE. \tag{5}$$

Inserting equation (5) into equation (1) and introducing the electron visibility spectrum

$$W(u,v;E)=\int_x\int_y N(x,y)\overline{F}(x,y;E)e^{2\pi i(ux+vy)}dxdy \tag{6}$$

and the new cross section

$$K(q,E)dq=\frac{1}{4\pi R^2}\int_{\epsilon=q}^{\infty} D(q,\epsilon)Q(\epsilon,E)d\epsilon, \tag{7}$$

we obtain the integral equation

$$V(u,v;q)=\int_{E=q}^{\infty} W(u,v;E)K(q,E)dE \tag{8}$$

which relates the count to the electron visibility spectra.
The two different ways to reconstruct the electron flux spectrum images $N(x,y)\overline{F}(x,y;E)$ starting from the measured X-ray count visibilities $V(u,v;q)$ can therefore be summarized as follow:

(i) for each photon energy ϵ, reconstruct the function $(x,y)\mapsto I(x,y;\epsilon)$ from equation (1) and then, for each pixel (x,y), invert equation (5). As already remarked before, this way is not efficient for two main reasons: the first one is the high computational cost due to the pixel-for-pixel inversion of equation (5). The second one is the low quality of the data in the inversion of equation (5), which is a more unstable problem with respect to the regularized inversion of the Fourier transform (1);

(ii) for each frequency pair (u, v), reconstruct the function $E \mapsto W(u, v; E)$ from equation (8) and then, for each electron energy E, invert equation (6). This choice proved to be more effective thanks both to the lower computational time required (the photon visibilities are typically sampled in at most 32 frequency pairs for each detector) and to the reliability of the data when the ill-posed problem (8) is solved.

3. Application to a real flare

In this section we show how to apply method (ii) to analyze the data collected by RHESSI during a real flare event. We selected a 1 minute-time interval around the emission peak of the 2002 April 15 flare (00:11:00 - 00:12:00 UT) and we used visibilities from detectors 3 through 9 in the energy interval $10 - 30$ keV with a sampling distance of 2 keV. Equation (5) has been deeply analyzed in several papers [4], [7], [10] and an inversion software based on the Tikhonov regularization method [13] has been implemented by the authors of this paper (and integrated in the official software of the mission) in order to obtain stable forms for $\overline{F}(x, y; E)$. From a purely methodological viewpoint, equation (8) is very similar to equation (5) and can be solved with the same software (after a modification of the integral kernel). Therefore, for each detector and each frequency pair (u, v) for which visibilities are available we constructed a X-ray count visibility spectrum $V(u, v; q)$ straightly from RHESSI data and applied our code to obtain the corresponding electron visibility spectrum $W(u, v; E)$. Thanks to the Tikhonov regularization procedure, from the knowledge of the X-ray count visibility spectrum up to 30 keV we are able to extract information on the electron visibility spectrum at energy values higher than 30 keV. In our case we found that good electron visibilities can be produced up to energy values near 50 keV. The regularized visibilities have been used as input to a Maximum Entropy algorithm [2] and 64×64 electron flux maps have been produced. We chose Maximum Entropy to invert equation (6) because is the method commonly used by the RHESSI community and is already implemented in the official software of the mission. In Figure 1 we give the electron maps corresponding to the energy intervals $10 - 12$, $14 - 16$, $18 - 20$, $22 - 24$, $26 - 28$, $30 - 32$, $34 - 36$ and $38 - 40$ keV.

Once we produced a set of electron flux images, we can easily select some peculiar regions of the sun and extract the corresponding electron flux spectra which are the quantities of central interest in the study of solar flares. In the case of the 2002 April 15 event, we chose two regions (labelled "Footpoint 1" and "Footpoint 2") corresponding to the footpoint sources and one other region (labelled "Middle") located approximately midway over the two footpoints. The regions selected are represented in Figure 2 on the electron image corresponding to the energy range $10 - 12$ keV. In Figure 3 we plot the electron flux spectra extracted from the three regions and averaged with respect to the area of the regions themselves. In order to calculate the error bars at each point of the spectra, we adopted the following procedure:

(i) the propagation error on the electron visibility spectra is calculated by means of a confidence strip [1], i.e., many different random realizations of the input photon visibility spectrum are realized and the corresponding regularized solutions are superimposed to determine a strip of reconstructed electron visibility spectra;

(ii) for each spectra of the strip we built the corresponding set of electron flux images through the Maximum Entropy algorithm and extracted the electron flux from the selected regions;

(iii) for each energy, the length of the error bar is given by the difference between the maximum and the minimum among the values of the flux obtained in step (ii).

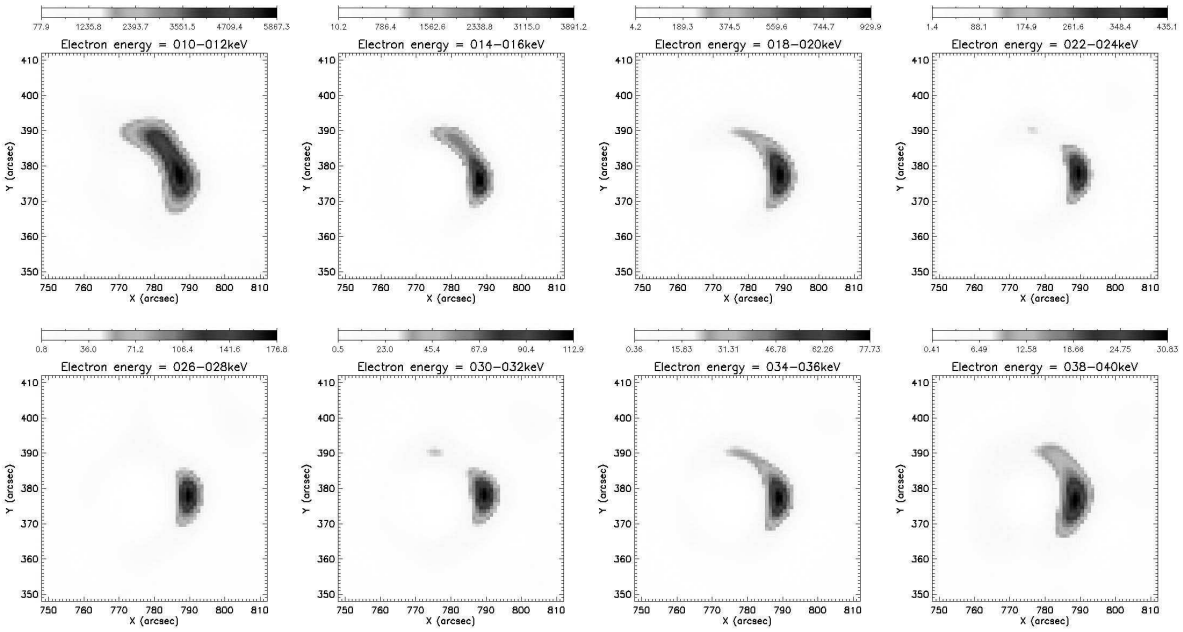

Figure 1. Electron flux images for the 2002 April 15 (00:11:00 - 00:12:00 UT) event for the energy intervals reported over the maps.

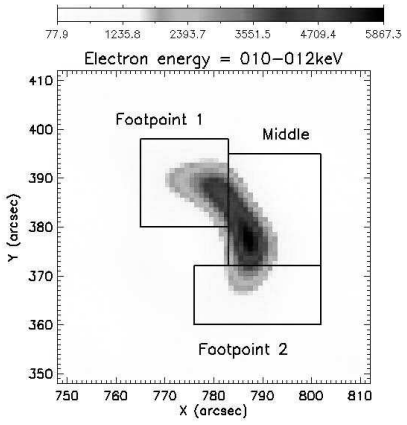

Figure 2. Electron image in the energy range $10-12$ keV with three subregions of interest labeled.

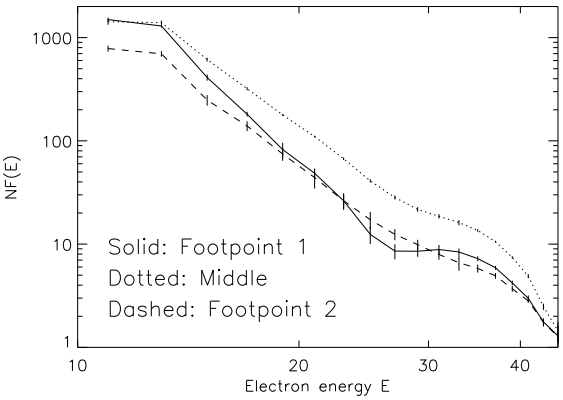

Figure 3. Electron flux spectra for the three subregions highlighted in Figure 2 (averaged by dividing for the areas of the regions).

4. Conclusions

In this paper we have illustrated a new algorithm for the reconstruction of two-dimensional electron flux maps at different electron energies starting from a set of X-ray count visibilities given by RHESSI. The method essentially involves a regularized inversion of each X-ray count visibility spectrum to obtain Fourier transforms of the electron flux maps at given frequencies. The reconstructed electron images are then achieved by means of a Fourier-based imaging reconstruction technique. The main improvement of the method with respect to traditional imaging spectroscopy techniques is that spatial maps of the electron flux for any given electron energy can be achieved starting from the best measurements available and in a reasonable

computational time. Our method has been applied in the case of a real flare (2002 April 15, 00:11:00 - 00:12:00 UT) and the electron flux maps have been produced in energy ranges beyond the ones available in the count domain. Electron flux spectra have been finally extracted from selected regions of interest of the reconstructed electron images and have been plotted together with the corresponding error bars for analysis and comparison.

Acknowledgments
The Swiss International Space Science Institute (ISSI) is kindly acknowledged.

References

[1] Bertero M 1989 *Linear inverse and ill-posed problems* In: P W Hawkes (Ed) Advances in Electronics and Electron Physics (New York, NY: Academic Press)
[2] Bong S C, Lee J, Gary D E and Yun H S 2006 *Astrophys. J.* **636** 1159
[3] Brown J C, Emslie A G and Kontar E P 2003 *Astrophys. J.* **595** L115
[4] Brown J C, Emslie A G, Holman G D, Johns-Krull C M, Kontar E P, Lin R B, Massone A M and Piana M 2006 *Astrophys. J.* **643** 523
[5] Hurford G J *et al* 2002 *Sol. Phys.* **210** 61
[6] Koch H W and Motz J W 1959 *Rev. Mod. Phys.* **31** 920
[7] Massone A M, Piana M, Conway A and Eves B 2003 *Astron. Astrophys.* **405** 325
[8] Mertz L N 1967 *Proc. Symp. on Modern Optics* v 17 of the Microwave Research Institute Symposia Series (Polytechnic Institute of Brooklyn - New York)
[9] Piana M, Massone A M, Hurford G J, Prato M, Emslie A G, Kontar E P and Schwartz R A 2007 *Astrophys. J.* **665** 846
[10] Piana M, Massone A M, Kontar E P, Emslie A G, Brown J C and Schwartz R A 2003 *Astrophys. J.* **595** L123
[11] Prince T A, Hurford G J, Hudson H S and Crannell C J 1988 *Sol. Phys.* **118** 269
[12] Schnopper H W, Thompson R I and Watt S 1968 *Space Sci. Rev.* **8** 534
[13] Tikhonov A N and Arsenin V Y 1977 *Solution of Ill Posed Problems* (Washington, D.C.: W H Winston)